Thermochimica Acta 502 (2010) 60–65

Contents lists available at ScienceDirect

Thermochimica Acta

journal homepage: www.elsevier.com/locate/tca

Thermal and rheological behavior of acetylacetone stabilized ZnO nanofluids

Vijay S. Raykar, Ashok K. Singh*

Department of Aerospace Engineering, Defence Institute of Advanced Technology, Deemed University, Girinagar, Sinhagad Road, Pune 411 025, India

ARTICLE INFO

Article history:
Received 15 June 2009
Received in revised form
21 December 2009
Accepted 5 February 2010
Available online 24 February 2010

Keywords:
ZnO nanoparticles
Acetylacetone
Rheology
Rheopectic
Effusivity

ABSTRACT

Acetylacetone (acac) ligand has been used for stabilization of ZnO NPs in water that form weak chelating complex which simultaneously breaks ZnO clusters, wrap and make ZnO NPs water soluble. Both thermal effusivity and conductivity show sigmoidal behavior over a temperature range of 283–323 K for low concentration fluids. The flow characteristics show rheopectic behavior according to concentration of ZnO NPs with highly non-Newtonian characteristics at lower shear stresses. Temperature dependence of the rheological characteristics suggests that above room temperature viscosity is higher for higher concentration nanofluid that can be attributed to agglomeration.

1. Introduction

Zinc oxide NPs exhibits remarkable physical properties that make metal oxide NPs as strong candidates in nanofluids and other applications [1]. Despite such an extraordinary heat transfer properties of oxide NPs there are still many issues to be resolved for their practical applications [2]. Key issues are insolubility and aggregation of oxide NPs in aqueous solutions due to their strong hydrophilicity and Van der Waals interactions which make practical applications very problematic [3]. In recent years, progress has been made in preparing dispersion of various oxide NPs in aqueous media using various dispersing agents such as surfactants, binders, polymers, etc. [4–6]. Nanofluids have been usually synthesized by dispersing oxide NPs in base fluids with sonication and encapsulating with dispersants. The dielectric constant of solvent also plays an important role in solubility of inorganic salts and NPs where higher polarity of solvent refers to greater solubility [7]. In the nanofluids using water, ethylene glycol as base media with metal NPs, oxide NPs with surfactant such as a cetyl trimethyl ammonium bromide (CTAB) and sodium dodecyl sulphate (SDS) have been selected to generate an electrical double layer, but other coordination complexes such as acac have received scarce attention in stabilization of nanoparticulate suspension [3]. Acac and its derivatives have been studied for their facile formation of stable complexes with metal oxides. The successful procedures for the synthesis of water soluble metal oxides have been reported for ZrO_2, TiO_2, etc., with acac [8]. Zaban and Grinis [5] prepared stable suspensions of TiO_2 NPs using uncharged metal oxide NPs treated with acac in polar organic solvents under ultrasonication and then utilized for electrophoretic deposition (EPD) process [5,8]. To authors knowledge there is no report on stable suspension of ZnO NPs in water using acac. To prepare stable nanofluids and controlling the aggregation of oxide NPs, in general, is still a challenge. The versatility of acac as coordinating ligand for aluminosilicate compounds is explained by Sohn and Lee [9]. Acac is well known bidentate ligand an oxo-bridged dimmer complexating single metal atom in two or more numbers [10]. For this reason passivation with very thin layer of non-ionic surfactant like acac is highly desirable. It is not only useful to prevent complete agglomeration but also breaks the ZnO nanocrystallites and distributes ZnO NPs uniformly throughout the solution. Recent publications have focused on determination of thermal conductivity and diffusivity of various nanofluids [11,12]. Thermal conductivity and diffusivity are two direct heat conduction indices that are used to describe thermal behavior of nanofluids [13,14]. Effusivity measures the nanofluids ability to exchange heat with surroundings, i.e. its utility in making complete thermal characterization of materials through a single parameter. At the best of authors knowledge there is no report on thermal effusivity of nanofluids. A measurement of thermal effusivity has been reported for liquids using photoacoustic technique with their focus on the measurement technique [15–19]. Castro et al. reported effusivity measurements for biodiesels using photothermal technique and found ester inclusion is responsible for the variation in effusivity [20]. George et al. measured effusivity values by photoacoustic technique for liquid crystal mixtures [18]. However, when using the photothermal and photoacoustic techniques the instrumentation

* Corresponding author.
E-mail addresses: aksingh@diat.ac.in, draksingh@hotmail.com (A.K. Singh).

0040-6031/$ – see front matter © 2010 Elsevier B.V. All rights reserved.
doi:10.1016/j.tca.2010.02.007

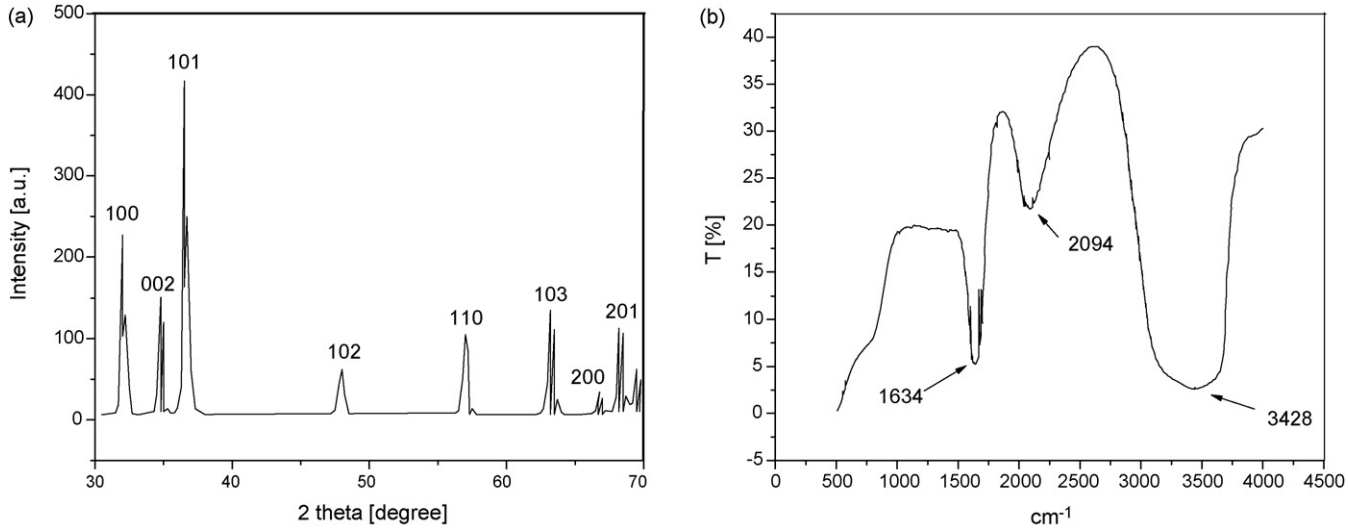

Fig. 1. XRD spectra of calcinated ZnO NPs (a) and FTIR spectra of ZnO NPs capped with acac (b).

required is very costly compared to the plane heat source technique which is very versatile and cheaper to design or fabricate. Recently, there has been significant interest in studying rheological and other flow properties of nanofluids for thermal applications [21]. Chen et al. [21,22] prepared TiO_2 nanofluids using ethylene glycol as base media and reported the Newtonian behavior of nanofluids and increased viscosity was explained because volume fraction and aggregation of NPs. Namburu et al. [23] has reported rheological behavior of CuO NPs in ethylene glycol at subzero temperatures, showing Newtonian behavior. However, they do not found rheopectic behavior of nanofluid. In this paper we propose a novel and simple method for the synthesis of water soluble ZnO NPs with a careful selection of acac amount to break ZnO clusters and make it water dispersible. Modifying NPs with acac precludes their aggregation and sedimentation in water. Moreover O–H groups on the surface of obtained ZnO NPs are reduced and perfect dispersion is achieved in water. The advantage of surface modification enhances suspension stability, reduces ZnO nanocrystallite size and the formation of very thin layer of non-ionic surfactant acac. Therefore, we are interested in knowing the effect of functionalization of zinc oxide NPs and different amount of particle loadings (in water) on their thermal and rheological properties.

2. Experimental

2.1. Materials

All chemicals were of reagent grade and were used without further purification. Zinc acetate dihydrate ($(CH_3COO)_2Zn{\cdot}H_2O$) were purchased from Aldrich. Acetylacetone ($C_5H_8O_2$) spectroscopic grade was purchased from Spectrochem Pvt. Ltd. Sodium hydroxide (NaOH) and tri ethanol amine (TEA) were purchased from Merk India Ltd.

2.2. Synthesis of ZnO NPs

Two solutions were prepared by dissolving 20 mg of $(CH_3COO)_2Zn{\cdot}H_2O$ (solution A) and 295 mg of NaOH (solution B) in 100 ml deionized water. Subsequently, solution B was added to solution A under vigorous stirring at 313 K for 20 min in microwave oven kept at medium level. Thereafter, 2 ml of TEA was added during vigorous stirring and thereafter temperature was kept at 333 K. After 30 min of heating, whitish colloidal solution has been obtained. The ZnO NPs were separated from the solution by centrifuging at 2000 rpm for 1 h. They were redispersed in ethanol and centrifuged again, and the procedure repeated for three times. The separated ZnO NPs calcined for 4 h at temperature of 973 K under normal conditions [24].

2.3. Synthesis of ZnO nanofluids

Three types of nanofluids were prepared by dissolving 75 mg (type I), 250 mg (type II) and 500 mg (type III) each in 100 ml of deionized water. These solutions were sonicated for 1 h and subsequently 3, 5 and 7 ml of acac is added in type I, II and III solutions and sonicated again for 10 min.

2.4. Characterization of ZnO NPs and nanofluids

The crystalline structure of the NPs was examined by X-ray diffractometer (Bruker AXS, Germany Model-D8) with Cu Kα radiation ($\lambda = 1.5418$ Å). The crystal phases of as synthesized ZnO nanopowders were determined by X-ray diffraction (XRD) patterns as shown in Fig. 1a. The diffraction pattern and interplane spacing has been well matched with that of structural database which further reveal formation of wurtzite nanocrystals (JCPDS file number: 080-0074) [25]. Presence of the carbonyl (carboxylation) groups of acac functionalized ZnO nanofluids was confirmed by Fourier transform IR (FTIR), as shown in Fig. 1b. A clear C=O stretching vibration at 1638 cm^{-1} appears in the spectrum of the carboxylated ZnO nanofluids (see Fig. 1b). The broad band between 3000 and 3600 cm^{-1} is a result of O–H absorptions from the water. The size and morphology of the ZnO NPs were determined using scanning electron microscopy (JEOL ASM 6360A). Fig. 2 shows typical scanning electron micrograph (SEM) images of ZnO NPs after calcinations. The SEM image shows randomly distributed ZnO NPs having non-spherical shape and diameter in the range of 100–150 nm, respectively. The average particle sizes of the ZnO NPs coated with acac were measured by particle size analyzer (Nicomp ZLS 380). Particle size measurement of ZnO nanofluids from dynamic light scattering (DLS) clearly indicates that the size of ZnO NPs have been reduced from 150 to 80 nm (approximately) in each case due to the reaction with acac as shown in Fig. 3a for nanofluid of type II. The reduction in ZnO size is presumably because of breaking of ZnO cluster aggregation. UV–vis absorption spectra of the nanofluids were recorded with high resolution

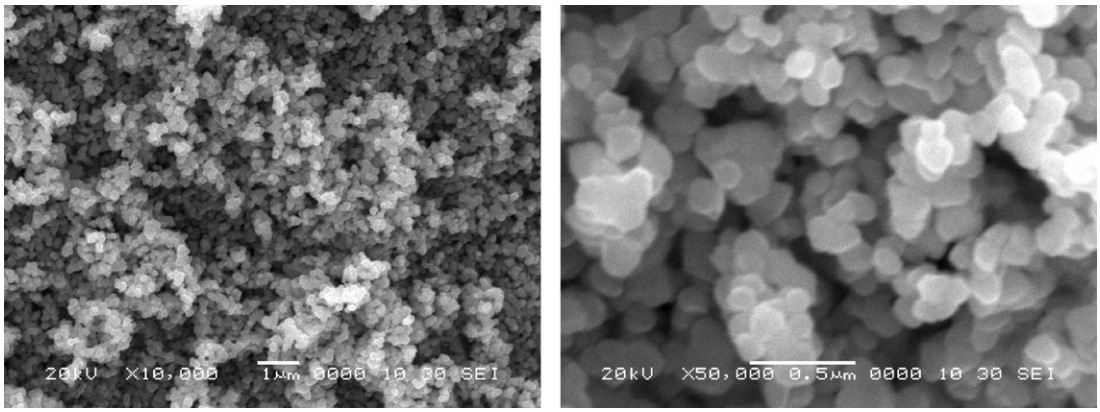

Fig. 2. SEM images of ZnO NPs.

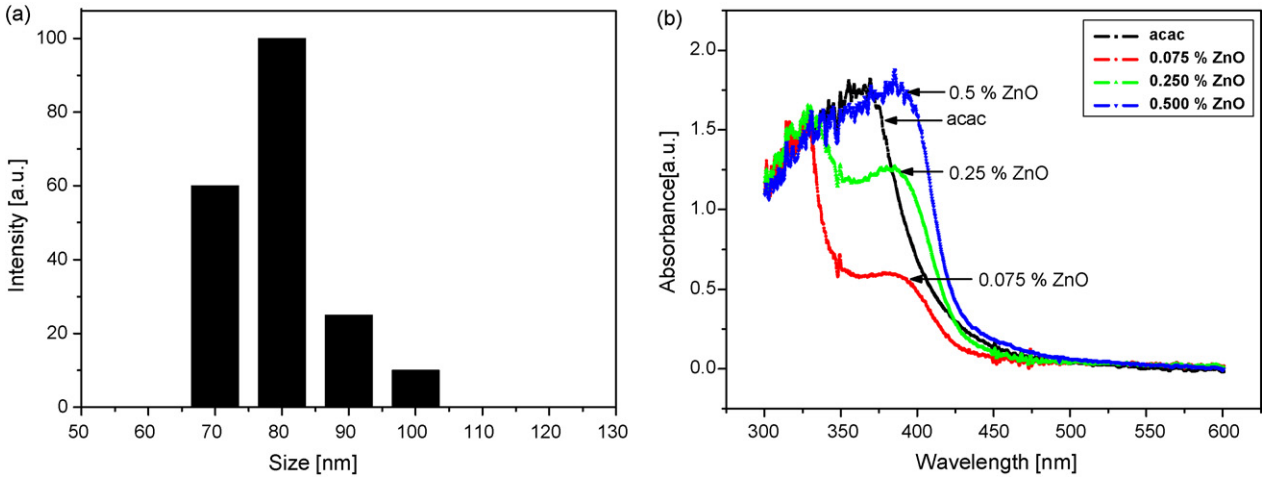

Fig. 3. Dynamic light scattering results (a) and optical absorption spectra of ZnO nanofluids (b).

spectrometer (ocean optics HR-400). Absorption spectra showed a broad absorption band of 300–500 nm with shoulder around 380 nm for all types of solutions with only variation in percentage of absorption, which could be attributed to percentage or concentration loading of ZnO NPs and provided additional evidence of the existence of single size distribution of ZnO NPs (Fig. 3b). The image in Fig. 4 compares the ZnO NPs dispersion in water before and after surface modification and shows that the modified ZnO NPs form transparent stable water dispersion. It can be clearly observed that the aggregation and sedimentation of NPs is prevented by modifying the ZnO NPs with acac. It also does not scatter the laser light visibly (Tyndall effect). All the three solutions have been found to be stable from date of preparation to as on date (over 9 months to 1 year). A rheological study of nanofluids was done using Rheologica Nova Rheometer with plate-plate geometry having plate diameter of 25 mm.

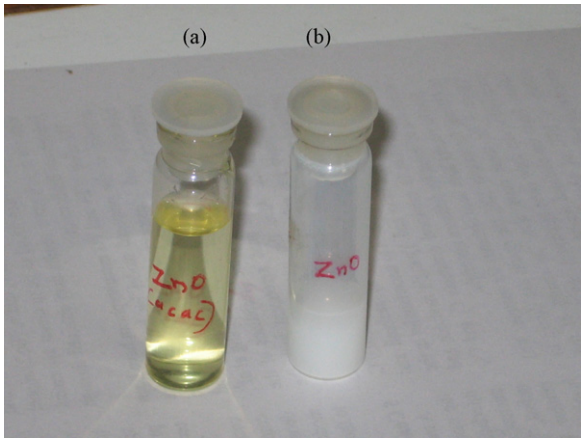

Fig. 4. Nanofluids after the addition of acetylacetone (a) and before (b).

2.5. Effusivity sensor fabrication and measurement

A plane heat source based effusivity sensor having radius of circle 25 mm was designed using insulated constantan wire. The heater so arranged is compressed between the two copper foils with the help of araldite and filled with silica insulation powder to reduce convection and a copper constantan thermocouple is placed at the center of heating coil. This assembly was compressed under heavy weight and kept for 2 days. Thereafter, this assembly was fixed between two bakelite rings having inner diameter of 48 mm and outer diameter 52 mm to reduce the heat losses [26]. The sensor is placed in the nanofluid sample inside a beaker. For a particular run a 45 mA of current was supplied through programmable power supply and temperature–time data were collected with the help of data acquisition system. From the slope of temperature time data effusivity of nanofluid was calculated [26] using Eq. (1):

$$e = \frac{q}{B_0\sqrt{\pi}} \quad (1)$$

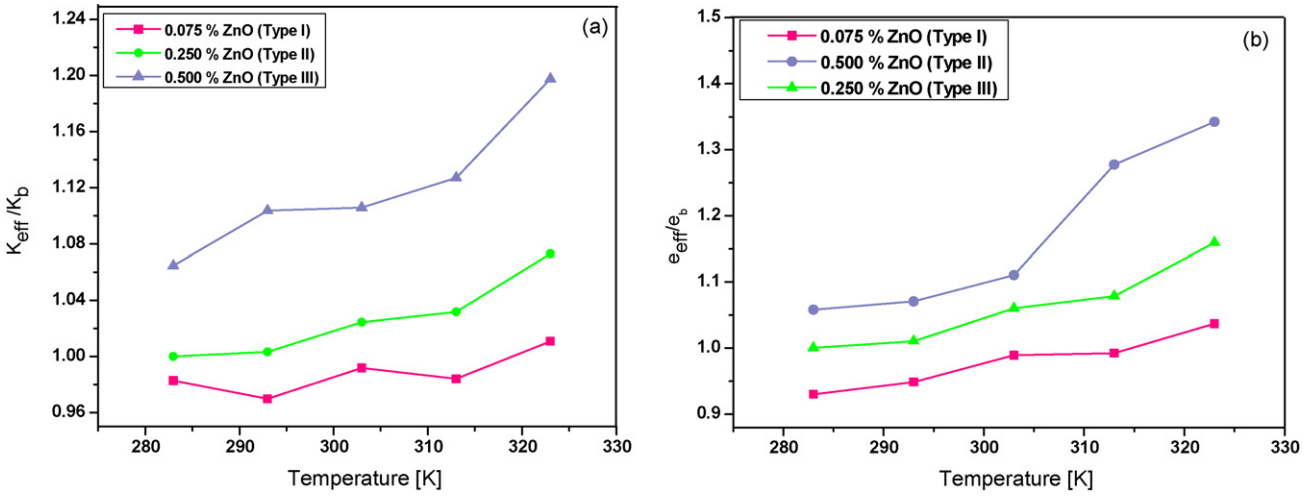

Fig. 5. Thermal conductivity (a) and effusivity (b) results for ZnO nanofluids.

where q is the input power and B_0 is slope between temperature–time data.

2.6. Thermal conductivity measurement

Transient hot wire method [27] was used to measure the thermal conductivity of nanofluids. The thermal conductivity can be calculated using Eq. (2):

$$k = \frac{q}{4\pi} \frac{\ln(t_2/t_1)}{T_2 - T_1} \quad (2)$$

where q can be taken as the input power per meter length of heating wire, T_1 and T_2 are temperatures at time t_1 and t_2, respectively. For measurement of effusivity and thermal conductivity, the container was filled with sample and the sensor was inserted at the center of the double walled container connected to constant temperature bath (Julabo F32 model) and allowed to equilibrate to bath temperature. After the initial temperature was recorded, current was supplied to the heater. The temperature versus time data was acquired using data acquisition system from which thermal conductivity was estimated.

3. Results and discussion

To understand thermal transport properties of ZnO NPs in water, thermal conductivity and effusivity measurements have been carried out on ZnO nanofluids. Hot probe method and plane heat source technique have been used for thermal conductivity and for thermal effusivity measurements, respectively [25,26]. Fig. 5a and b, respectively, shows variation of thermal conductivity and effusivity ratio with temperature for type I (0.075% ZnO), type II (0.25% ZnO) and type III (0.5% ZnO) nanofluids. The thermal conductivity and effusivity values of each nanofluid are obtained by sweeping the temperature from 283 to 323 K. All solutions exhibit enhanced heat transfer characteristics with temperature [26], except for type I nanofluid. As can be seen from figure both thermal conductivity (k) and effusivity (e) increases with temperature. Thermal conductivity exhibits slow increase for I and II nanofluids while type III nanofluid shows relatively fast increase in k for the given temperature range. Beyond 303 K temperature, the k and e is found to increase abruptly for nanofluid of type III, which can be attributed to agglomeration of ZnO NPs. At higher temperature acac in the solution of type III is not able to hold the ZnO NPs in dispersed condition and results in agglomeration. Beyond 323 K the nanofluid starts evaporating and ZnO starts to deposit on the wall of glass beaker in which measurements have been carried out. In case of type III solution with increases in temperature 303 K onwards, solvent molecules become free and leading to agglomeration of ZnO NPs. One can say that nanofluid has separated into solid and liquid phase. Moreover, evaporation increases rapidly with increase in temperature and has been observed during experiments. Therefore higher loading of ZnO NPs and evaporation are jointly responsible for agglomeration in type III solution. In type II and I solution loading of ZnO NPs being less and acac is able to hold NPs in well dispersed phase for given the temperature range. Above about 323 K it has been observed that all the solutions start showing agglomeration with significant evaporation.

This highly agglomerated ZnO, in case of nanofluid of type III, forms a non-uniform coating over thermal conductivity probe and effusivity sensor which gives out high values of thermal conductivity and effusivity. The measured thermal conductivity and effusivity values for water at room temperature (303 K) are 0.61 (W/mK) and 1580 ($J\,m^{-2}\,K^{-1}\,s^{-1/2}$), respectively. The normalized k and e values (by that of base fluid) at temperature 303 K are 0.9918, 0.9893, 1.024 and 1.06, 1.105 and 1.110 for type I, II and III nanofluids, respectively. Thermal property of water is not only affected by addition of ZnO NPs but also due to surfactant (acac) (being constituent phase of nanofluid). In case of type I solution added acac is 3 ml, i.e. 3% by volume. It also lowers the effusivity of solution as compared to increment due to added ZnO NPs. Acac is having very low effusivity ($558\,J\,m^{-2}\,K^{-1}\,s^{-1/2}$ obtained from k and volumetric heat capacity [26]) in comparison to water ($1580\,J\,m^{-2}\,K^{-1}\,s^{-1/2}$) and responsible for decrement in effusivity of ZnO nanofluid of type I. In type II and III case the effect of particle loading is significant as compared to added acac. Certain amount of variation in thermal property in type I solution may also be due to measurement uncertainty.

Nanofluids using ZnO modified by acac showed heat transfer enhancement for solutions of type II and III. However, higher concentration nanofluid of type III is not suitable for heat transfer application as it settles down, agglomerates and forms a coating inside the container in which tests are carried out.

In order to study flow properties of the ZnO nanofluids, plate–plate geometry configuration of rheometer has been used. The typical flow characteristic of each nanofluid is obtained by sweeping the stress from 0 to 10 Pa. Fig. 6a and b shows typical flow characteristics for ZnO nanofluids on normal and logarithmic scales. All nanofluids exhibit analogous flow characteristics for high stresses. For nanofluid of type I the shear rate increases linearly with stress. When the stress is increased, the shear rate exhibits a

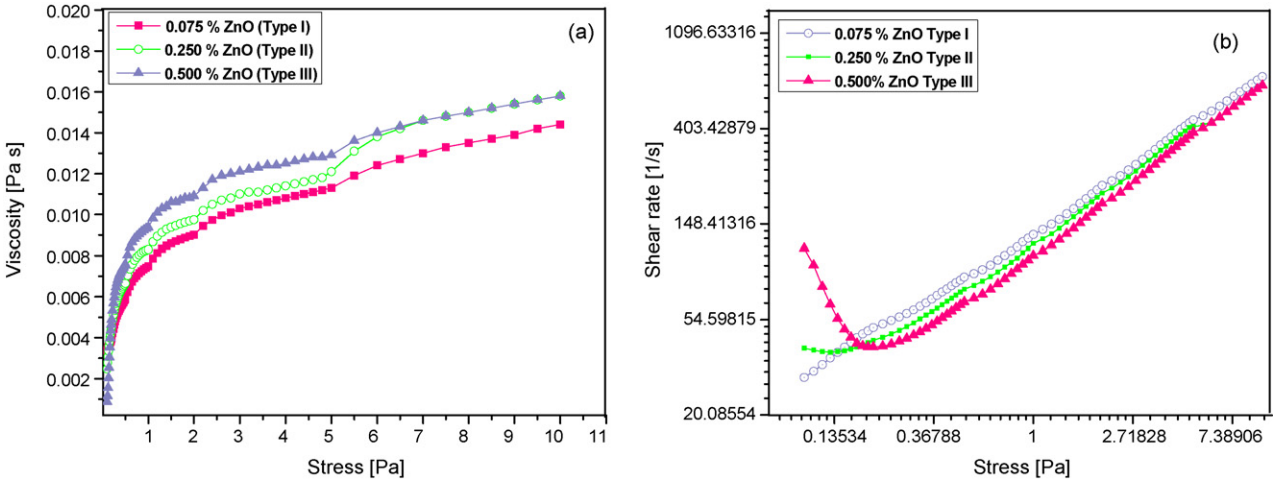

Fig. 6. Flow properties of ZnO nanofluids: (a) viscosity variation with stress and (b) plot on natural logarithmic scale.

local non-linear behavior between 0.1 and 0.2 Pa stress value for the nanofluids of type II and III whereas sample I shows more or less linear behavior. Beyond this value, the shear rate–stress curve shows a regime of rheopexy for a range of stress from 1 to 10 Pa [28,29]. For further increment of stress the nanofluids are being thrown out from the plate–plate geometry configuration. The typical increase in viscosity observed for a read-out stress of 0.1–0.2 Pa is from 3.356 to 3.975 mPa s, 2.468 to 4.543 mPa s and 0.866 to 4.89 mPa s for nanofluids of type I, II and III, respectively. For dilute dispersion (type I) with 0.1–0.2 Pa stress range the linear behavior can be explained based on weakly bonded particle aggregation forming a dispersed suspension with near Newtonian behavior as shown in Fig. 6b. The linear state has drastically changed to non-linear state for higher loading of ZnO NPs.

These results suggest that there is a rapid increase in viscosity for higher loading and at lower stress rates. The effect of the non-linear increase in the viscosity at low stresses for higher loading can be explained with the help of yield stress characteristics shown in Fig. 7a and reveal that the nanoparticle suspension begins to flow only after the applied stress exceeds certain critical value, know as the yield stress [30]. This value is approximately 0.27 Pa for type III nanofluid. The effect of agglomeration/cluster formation starts from the initial value of stress showing cluster formation at faster rate up to the stress value of 0.2 Pa beyond which nanofluid begins to flow showing saturated viscosity type of behavior. For the low concentration samples (nanofluid of type I and II) there is small amount of cluster formation as seen from small rise in viscosity while for nanofluid of type III viscosity increase is higher as can be seen from lower shear rate values for applied stress below 0.2 Pa. After yield stress all nanofluids show more or less linear increase in shear rate with stress yielding slight increase in viscosity which can be accounted for rheopectic nature of nanofluids as shown in Fig. 7b.

Further information about the agglomeration/cluster formation mechanisms can be obtained from temperature-dependent viscosity measurements. Fig. 8 shows the viscosity measured at 0.2 Pa stress as a function of temperature for all nanofluids. The initial rapid decrease in viscosity from 283 to 288 K can be explained by a well dispersed phase of ZnO NPs that exist for all the three nanofluids at low temperature, while the viscosity for nanofluids of type I and II is almost temperature-independent within the temperature range of 288–323 K. The viscosity–temperature curve for nanofluid of type III beyond the room temperature shows an interruptible behavior as shown in Fig. 8. This interruptible behavior in viscosity above room temperature shows an almost non-linear-dependence on applied temperature indicating the viscosity increase is dominated by solvent evaporation and concentration of ZnO NPs. In contrast, there is slight decrease in viscosity for type I and II

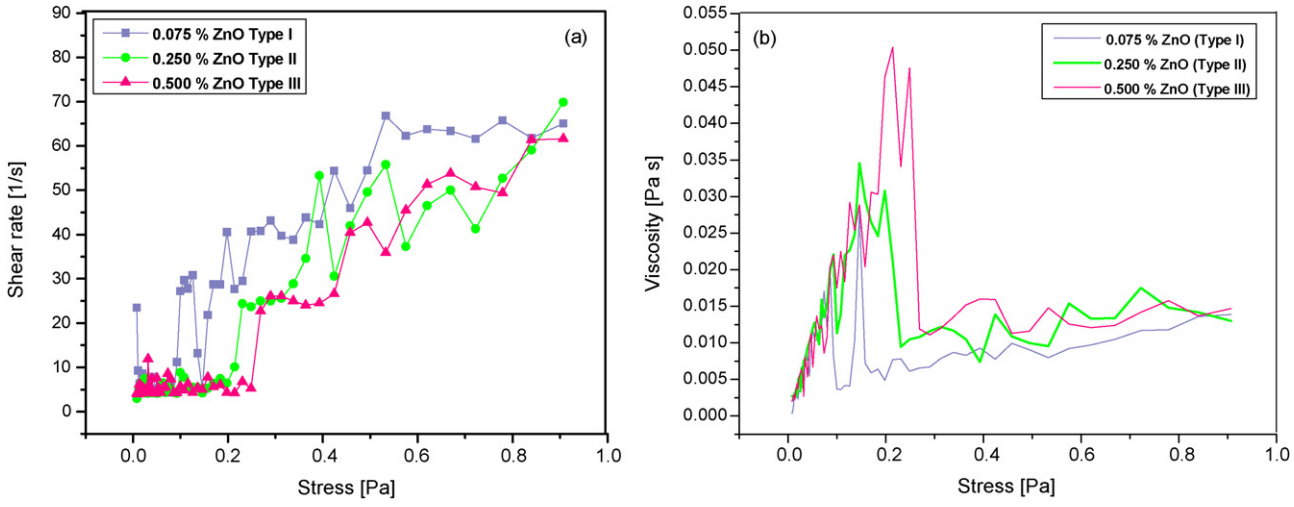

Fig. 7. Yield characteristics of ZnO nanofluids: (a) yield stress and (b) viscosity variation with stress.

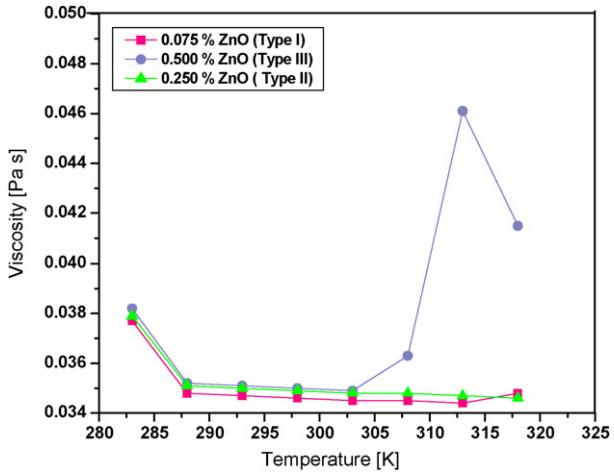

Fig. 8. Viscosity variations of ZnO nanofluids with temperature.

nanofluids. As evaporation increases with increases in temperature above 323 K, viscosity is expected to increase with an interruptible behavior because of the loss of solvent above this temperature. This suggests that the lower concentration nanofluid (type I and II) have the constant viscosity (or slight decrease without solvent evaporation) governed by stable dispersion of suspension for given temperature range. In contrast, below room temperature all the nanofluids show almost constant viscosity. Whereas the viscosity of higher loaded nanofluid of type III deviates almost 10 mPa s at a temperature of 313 K from room temperature viscosity. This behavior can be explained by the agglomeration of ZnO NPs as rate of evaporation of solvent increases with increase in temperature above room temperature (303 K onwards).

4. Conclusions

Water soluble ZnO NPs have been synthesized and the effect of ZnO NPs loading and temperature on thermal and rheological behavior of ZnO nanofluids has been investigated. Acetylacetone have been used as functionalizing agent to prepare water soluble ZnO NPs. The adsorption of acac on ZnO NPs exhibits reduction of particle size from approximately 150–80 nm, respectively. For higher loading of ZnO NPs (0.5 wt.% and above) in water the amount of acac added is not been able to prevent agglomeration of NPs. Researchers have given much attention on thermal conductivity rather than thermal effusivity of nanofluids. This investigation presents combined study of thermal conductivity and effusivity of nanofluids. An optimal enhancement of 2%, at room temperature, in thermal effusivity and conductivity with respect to water was discovered at about 0.25 wt.% loading. The results indicate that for higher loading of ZnO NPs aggregation could result in increment in thermal effusivity and conductivity of ZnO nanofluids. All studied nanofluids show non-linear rheological behavior (rheopecticity) with the 0.5 wt.% loaded nanofluid exhibiting the largest non-linearity in viscosity. This non-linearity is attributed to the effect of the agglomeration. Nanofluid with low weight percent loading close to or below the yield stress value showed almost linear behavior as exhibited by Newtonian fluid. The highly agglomerated state of higher loaded ZnO NPs was also demonstrated by viscosity studies which indicate interruptible increase in viscosity above room temperature while viscosity of samples remains unaffected below room temperature. The present approach may be explored for the synthesis of similar water soluble metal oxide NPs by proper selection of functionalizing agents with particle size tuning. The overall thermal and rheological results indicate that ZnO nanofluids could be used as a coolant below 0.5% loading of ZnO NPs in water with acetylacetone as a ligand for stabilization of suspension.

Acknowledgement

Authors are thankful to Vice Chancellor, Defence Institute of Advanced Technology (DIAT), Deemed University, Girinagar, Pune-411025, India, for granting permission to publish this work.

References

[1] S.H. Kim, S.R. Choi, D. Kim, Trans. ASME 129 (2007) 298.
[2] Y. Hwang, J.K. Lee, C.H. Lee, Y.M. Jung, S.I. Cheong, C.G. Lee, B.C. Ku, S.P. Jang, Thermochem. Acta 455 (2007) 70.
[3] X. Li, D. Zhu, X. Wang, J. Colloid Interface Sci. 310 (2007) 456.
[4] H.M. Xiong, Y. Xu, Q.G. Ren, Y.Y. Xia, J. Am. Chem. Soc. 130 (2008) 7522.
[5] A. Zaban, L. Grinis, A. Ofir, IPC8 Class: AH01B102FI, USPC Class: 2525195.
[6] V. Trisaksri, S. Wongwises, Renew. Sustain. Energy Rev. 11 (2007) 512.
[7] D. Sun, M. Wong, L. Sun, Y. Li, N. Miyatake, H. Sue, J. Sol Gel Sci. Technol. 43 (2007) 237.
[8] M.J. Santillan, F. Membrives, N. Quaranta, A.R. Boccaccini, J. Nanopart. Res. 10 (2008) 787.
[9] J.R. Sohn, S.I. Lee, Langmuir 16 (2000) 5024.
[10] P.A. Connor, K.D. Dobson, A.J. McQuillan, Langmuir 11 (1995) 4193.
[11] X. Zhang, H. Gu, M. Fujii, Exp. Therm. Fluid Sci. 31 (2007) 593.
[12] X.Q. Wang, A.S. Mujumdar, Int. J. Therm. Sci. 46 (2007) 1.
[13] M.J. Assel, I.N. Metaxa, K. Kakosimos, D. Constantinou, Int. J. Thermophys. 27 (2006) 999.
[14] X. Zhang, H. Gu, M. Fujii, Int. J. Thermophys. 27 (2) (2006) 569.
[15] J. Balderas-Lopez, Rev. Sci. Instrum. 78 (2007) 64901.
[16] R.S. Quimbay, Y.S. Chang, Rev. Sci. Instrum. 55 (8) (1984) 1287.
[17] A. Sikorska, B.B.J. Linde, W. Zwirbla, Chem. Phys. 320 (2005) 31.
[18] S.D. George, A.K. George, P. Radhakrishnan, V.P.N. Nampoori, C.P.G. Vallabhan, Smart Mater. Struct. 16 (2007) 1298.
[19] X. Wang, H. Hu, X. Xu, Trans. ASME 123 (2001) 138.
[20] M.P.P. Castro, A.A. Andrade, R.W.A. Franco, P.C.M.L. Miranda, M. Sthel, H. Vargas, R. Constantino, M.L. Baesso, Chem. Phys. Lett. 411 (2005) 18.
[21] H. Chen, Y. Ding, C. Tan, New J. Phys. 9 (2007) 367.
[22] H. Chen, Y. Ding, Y. He, C. Tan, Chem. Phys. Lett. 444 (4–6) (2007) 333.
[23] P.K. Namburu, D.P. Kulkarni, D. Misra, D.K. Das, Exp. Therm. Fluid Sci. 32 (2007) 397.
[24] N.F. Hamedani, F. Farzaneh, J. Sci. Islam. Repub. Iran 17 (3) (2006) 231.
[25] L. Guo, S.H. Yang, C. Yang, P. Yu, J. Wang, W. Ge, G.K.L. Wong, Chem. Mater. 12 (2000) 2268.
[26] L.S. Verma, A.K. Shrotriya, U. Singh, D.R. Chaudhary, J. Phys. D: Appl. Phys. 23 (1990) 1405.
[27] A.K. Singh, V.S. Raykar, Colloid Polym. Sci. 286 (2008) 1667.
[28] C. Oelschlaeger, G. Waton, E. Buhler, S.J. Candau, M.E. Cates, Langmuir 18 (2002) 3076.
[29] X. Yuan, M. Schnell, S. Muth, W. Schartl, Langmuir 24 (2008) 5299.
[30] L.F. Hakim, D.M. king, Y. Zhou, C.J. Gump, S.M. George, A.W. Weimer, Adv. Funct. Mater. (2007).